

Tribological performance of thermal sprayed coatings under abrasive conditions

Emmanuel GEORGIU ^{1,*}, Angelos KOUTSOMICHALIS¹, Dirk DREES ², Christos PANAGOPOULOS ³

¹ Hellenic Air Force Academy, Athens, Greece

² Falex Tribology, Rotselaar, Belgium

³ National Technical University of Athens, Athens, Greece

*Corresponding author: emmanouil.georgiou@hafa.haf.gr

Keywords

thermal spraying
coatings
abrasion
wear
friction
triboscopy

Abstract

In this work, the tribological behaviour of thermally sprayed titanium and chromium ceramic-based coatings was investigated under abrasive conditions. Their structure was studied by a scanning electron microscope (SEM), while their hardness was evaluated using a microhardness tester. To study the strength of these ceramic coatings under abrasion conditions, reciprocating sliding experiments were carried out in a high-precision (10 mN resolution, 1000 Hz data acquisition) pin-on-disk apparatus and by using a Ø 6 mm corundum ball to generate high contact pressures (1.5 GPa). To thoroughly investigate the friction evolution of the tribo-system, three-dimensional mapping of the tangential friction forces (triboscopy) was performed. Following the abrasion experiments, the wear of these coatings was measured using confocal microscopy. The obtained friction and wear results were compared to state-of-the-art materials and coatings that are currently being used in various industrial applications. From this comparison, it was found that the titanium and chromium ceramic-based coatings have comparable if not better tribological properties for the given conditions. The main wear mechanism was mainly two-body abrasion due to the surface roughness of the counter-material, as well as three-body abrasion due to the formation of debris at the interface.

History

Received: 16-02-2023

Revised: 16-03-2023

Accepted: 17-03-2023

1. Introduction

Thermal spraying has been present for more than a century since it was initially introduced in the early 1900s by Dr. Schoop [1]. During this time, it has evolved and improved to deposit a variety of metallic, ceramic, polymeric and composite materials, and is nowadays recognised as a reliable and cost-efficient method for depositing thick coatings onto industrial components [2]. Examples of thermal sprayed coatings can be found in a variety of industrial and technological fields that range from aerospace [3], automotive [4] and biomedical [5] components, up to vital parts in manufacturing processes [6] and energy production

[7]. Recently, thermal spraying is also considered a promising alternative to hard chromium coatings [8], in an effort to minimise the negative environmental impact of hard chromium electroplating processes [9].

Among the thermal spraying coatings, ceramic-based are gaining increasing importance as they can successfully protect metallic substrates from wear [10], oxidation [11] and corrosion [12]. However, one of their main drawbacks is that due to their high melting temperature and low thermal expansion (compared to the metallic substrate), they require a bond coating [13].

From the existing oxides, chromium oxide is the hardest and has also been reported to exhibit good frictional properties, high wear, and corrosion resistance [14]. Thus, it is used in tribological and microelectronic applications and as an adiabatic

material in aeronautics and space fields [14]. In addition, titanium oxide coatings because of their physical, chemical and electrical properties are used as hydrogen and oxygen sensors, self-cleaning and photocatalytic surfaces, and electron emitters for light emitting devices [15]. Despite the well-established and beneficial usage of these coatings, there is still a lack of information on their tribological behaviour. This derives from the fact that friction and wear are system properties that can considerably vary depending on the contact conditions, geometry, counter-material, environment etc. Therefore, in this work, the tribological performance of chromium- and titanium-based oxide coatings was evaluated under abrasive sliding conditions. The aim is to establish a structure-property relation and to understand the dominant wear mechanism that affects their tribological performance under the selected conditions. Finally, a comparison with state-of-the-art materials that are currently being used in various industrial applications was also made in order to see how these coatings rank in terms of friction and wear.

2. Experimental part

Commercially available chromia (Metco 106) and titania powders (Amperit 782) were deposited onto flat parallel steel substrates (Fe-0.60C-0.40Si-0.75Mn-0.035P-0.0035, wt. %). The chromia powder ($95\text{Cr}_2\text{O}_3$ - 4.25TiO_2 - $0.25\text{Fe}_2\text{O}_3$ - 0.5SiO_2 - $0.25\text{Al}_2\text{O}_3$ - 0.5Other , wt. %) had a particle size distribution of $-90/+11\ \mu\text{m}$, while the titania powder (99TiO_2 - $0.25\text{Fe}_2\text{O}_3$ - 0.3SiO_2 , wt. %) had particle size distribution of $-90/+45\ \mu\text{m}$.

Prior to spraying the steel substrates were grit blasted by alumina with 0.8 – 1 mm grain sizes to achieve an average roughness of about $8\ \mu\text{m}$. After sandblasting, the steel samples were cleaned in an ultrasound bath with acetone for 5 min and dried with compressed air. Then they were vacuum packed and conserved in a dryer at $60\ ^\circ\text{C}$ until coating deposition. To improve adhesion between the oxide-based coatings and the metallic substrate, a $100\ \mu\text{m}$ thick nickel aluminide (Metco 404NS) layer was used as a bond coating. Afterwards, $350\ \mu\text{m}$ chromia and $100\ \mu\text{m}$ titania coating were deposited by an APS gun (FST SG-100, 80 kW) fitted to a KUKA robotic arm. The spraying conditions selected based on previous research [16] are the following. For the deposition of chromia coatings, the voltage was 37.5 V, the

current 600 A, the argon pressure 120 psi, the hydrogen pressure 11 psi, the spraying distance was set at 100 mm, the spraying rate was 450 mm/s and a step of 5 mm was selected. For the deposition of titania coatings, the voltage was 38.5 V, the current 500 A, the argon pressure 120 psi, the hydrogen pressure 11 psi, the spraying distance was set at 100 mm, the spraying rate was 450 mm/s and a step of 5 mm was selected. To improve the adhesion between the substrate and the coating, an intermediate Ni-Al bond coating was sprayed with a voltage of 50 V, current of 450 A, argon pressure of 120 psi, hydrogen pressure of 9 psi, spraying distance of 100 mm, spraying rate of 450 mm/s and a step of 5 mm.

A JEOL JSM-63000 scanning electron microscope (SEM) was used for the microstructural analysis and to measure the thickness of the coated samples. The Vickers microhardness of the coatings was measured by performing 10 independent measurements in their cross-section with a Wolpert Wilson 402 MVD instrument.

The reciprocating sliding tests were performed under dry conditions with a Basalt-N2 tribometer (Fig. 1a). The applied load and tangential force are picked up by a high-precision displacement measurement of the spring elements (Fig. 1b), measured by capacitance sensors (resolution of $1/10.000$ of full scale, which is 10 mN for the 100 N sensor and a sampling rate of 1000 Hz). For the selected tests a normal force of 10 N, a displacement of 2 mm and a steady-state speed of 20 mm/s for 10,000

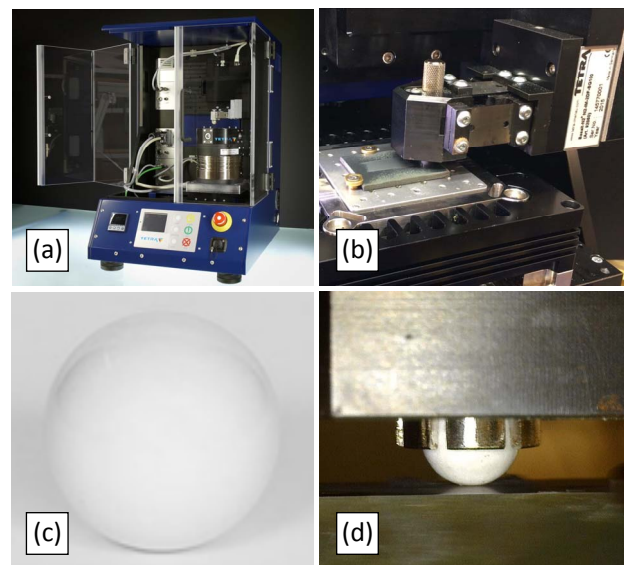


Figure 1. Reciprocating sliding testing: (a) Basalt-N2 tribometer, (b) spring sensor, (c) corundum counter-body material and (d) tribological contact

cycles (sliding distance 40 m) were selected. A commercially supplied $\varnothing 6$ mm corundum ball, with a hardness of 2000 HV 0.5 and a $Ra = 0.2 \mu\text{m}$, was used as a counter-body material (Fig. 1c). The resulting contact (Fig. 1d) was a point contact, generating an initial pressure of 1.5 GPa, a contact radius of $30 \mu\text{m}$, a maximum shear stress of 370 MPa and an interaction depth of about $30 \mu\text{m}$ (as calculated with HerzWin software). This means that in all tribotests the interaction volume is well within the bulk of the coating and not close to the interface or the substrate. Thus, the obtained results and relative ranking are not influenced by the different thicknesses of these two sprayed coatings.

Prior to the reciprocating sliding tests, the coated specimens were polished with SiC papers (up to P2500 grit) to an average surface roughness of approximately $0.3 \mu\text{m}$, as measured with confocal microscopy. Then both the coated samples and counter-body materials were cleaned in a heptane bath for 5 min with ultrasonic cleaning. All reciprocating sliding tests were performed at least three times from which the mean values were calculated. To explore the applicability of these coatings, tribological tests were also performed for the same test conditions on some commercially supplied industrial materials, namely Haynes 188 alloy (Co-22Ni-22Cr-14W-2.5Fe-1Mn-0.3Si-0.15C-0.04La-0.02P-0.015S, wt. %), Hardox 400 alloy (Fe-0.15C-0.6Si-1.2Mn-0.3Cr-0.25Ni-0.25Mo, wt. %), ASP 23 alloy (Fe-1.28C-4.2Cr-5Mo-6.4W-3.1V, wt. %), electrodeposited hard Cr [9] and ion beam assisted deposition Graphite DLC [17] coatings on ASP 23 substrates.

The wear mechanisms were analysed with a FEI XL 30 SEM and an Olympus B071 optical microscope (OM), which was connected to an energy dispersive X-ray analyser (EDS) apparatus. Wear loss was evaluated with a NanoFocus μSurf Explorer confocal microscope using a $10\times$ magnifying lens (200–400 confocal images captured per second and resolution in the z-axis, which is the height of topographical features, is in the nm range).

3. Results and discussion

Typical cross-sections of the as-sprayed titania and chromia coatings are presented in Figure 2. Dense coatings with a thickness of about $850 \mu\text{m}$ for chromia and $100 \mu\text{m}$ for titania were achieved. Limited cracks or flaws were observed at either the

interface between the sprayed coating and the substrate or between the sprayed splats. This indicates that a satisfactory adhesion was achieved. In addition, the microhardness of the chromia coating was $1190 \pm 120 \text{ HV } 0.5$, whereas for the titania $812 \pm 57 \text{ HV } 0.5$.

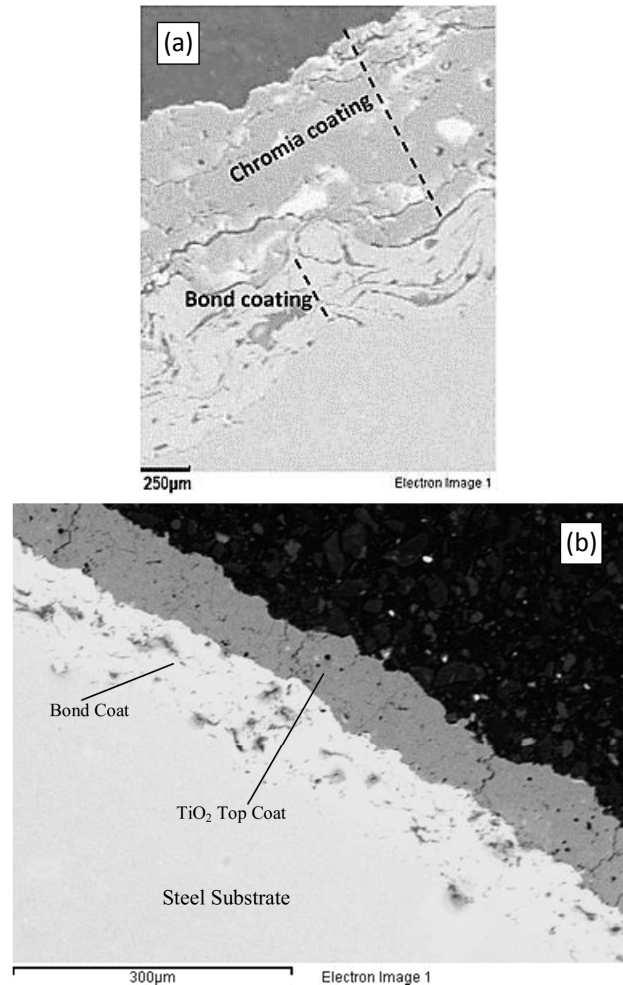


Figure 2. Cross-section images of as-sprayed: (a) chromia coating and (b) titania coating (reprinted from Koutsomichalis et al. [16], licensed under CC BY 4.0)

Figure 3 shows the evolution of the average coefficient of friction per cycle of chromia and titania coatings versus corundum. The triplicate tests appear to be very repeatable, especially after the running-in period, which indicates that: (a) these materials are exhibiting tribological homogeneity and (b) no significant changes in the wear mechanism occurred. The fluctuations during run-in are attributed to changes in the initial surface topography (asperities). As these topographical features are gradually removed, friction stabilises. In addition, the average coefficients of friction values between the two coatings appear to be similar.

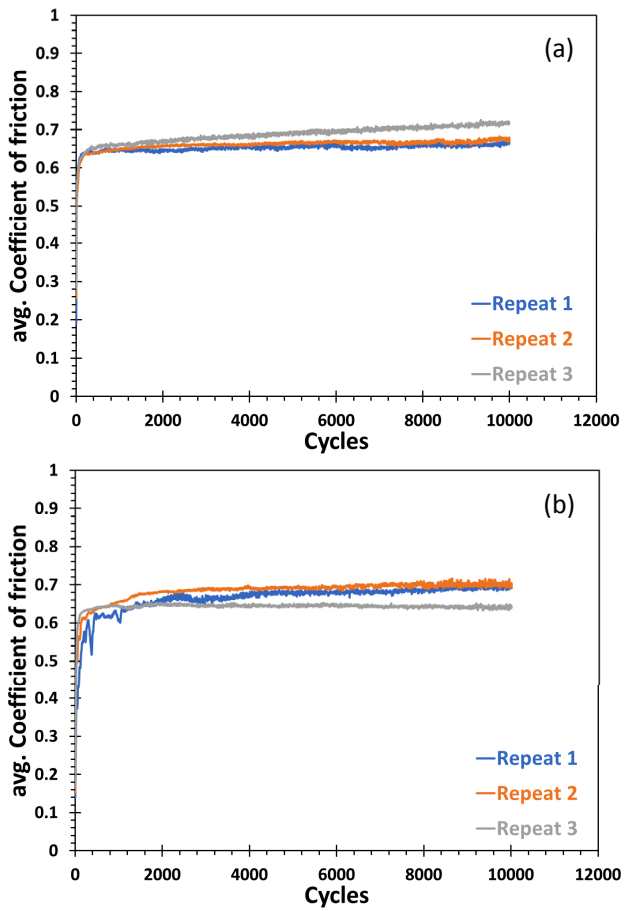


Figure 3. Evolution of average coefficient of friction per cycle of thermal sprayed coatings vs. \varnothing 6 mm corundum ball (10 N, 20 mm/s, 2 mm, 10.000 cycles): (a) chromia coating and (b) titania coating

To get a better insight into the evolution of friction during these tests, the 3D triboscopy patterns were analysed. In this 3D representation, the evolution of friction within each sliding cycle and throughout the whole test is stored. Indicative examples for the two coatings are given in Figure 4. It can be seen that despite the fact that chromia and titania coatings had a similar evolution of average coefficient of friction (Fig. 3) their 3D pattern are very different (Fig. 4). In particular for chromia coating a higher fluctuation of the friction force is recorded during each cycle, whereas the pattern of titania coating appears smoother. Peaks of friction are observed at the edges of the sliding loops especially for the chromia coatings, due to debris pile-up (Fig. 5a) that can lead to localised sticking phenomena [18].

This fluctuation is possibly linked to the generation of debris particles in the contact. Indeed, SEM images of the wear track revealed a high density of debris at the edges and within the chromia sprayed coated wear track (Figs. 5a, 5b and 6b). In addition, the morphology of the wear

track indicates that for both coatings the main wear mechanism is mainly abrasion (Figs. 5b, 5c and 6). In particular, at the beginning a two-body abrasion takes place due to the surface roughness of the counter-body material (ploughing lines along sliding direction), followed by three-body abrasion due to the formation of debris at the interface [19].

EDS analysis on the debris showed that they consisted mainly of worn and/or plucked out particles from the coating and some Al traces from the counter-body material. In particular, the chemical of the debris formed on the chromia coating was (in wt. %) 42.6 Cr, 7.9 Al and O as balance, and for the titania coating, it was (in wt. %) 42.1 Cr, 6.5 Al and O as balance. For the titania coatings, localised micro-cracks were also observed (Fig. 5d). The formation of micro-cracks can be linked to fatigue wear [20].

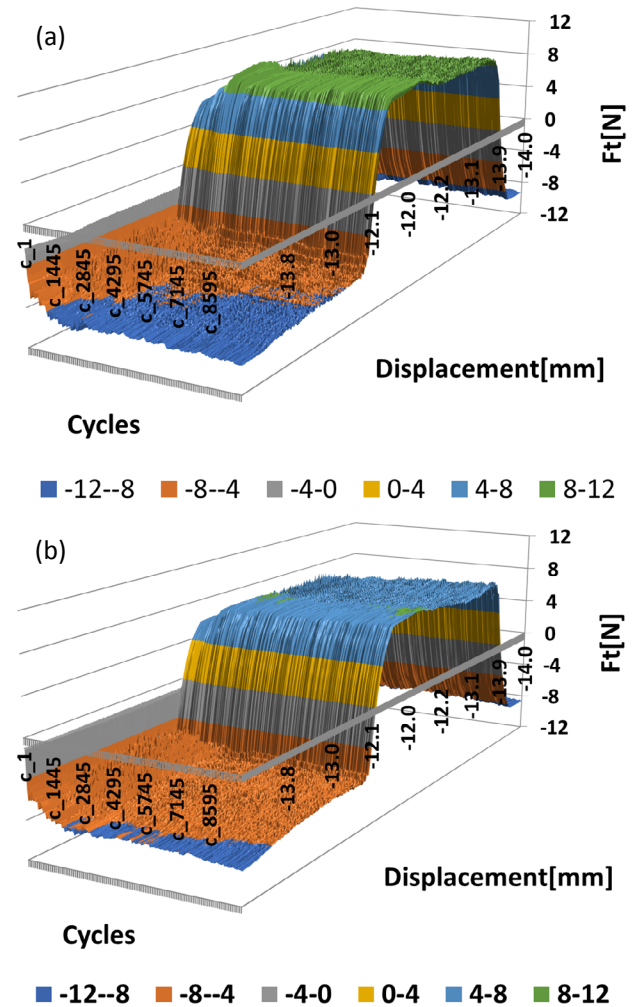


Figure 4. Example of 3D triboscopy pattern showing the evolution of frictional force during every sliding cycle for thermal sprayed coatings vs. \varnothing 6 mm corundum ball (10 N, 20 mm/s, 2 mm, 10.000 cycles): (a) chromia coating and (b) titania coating

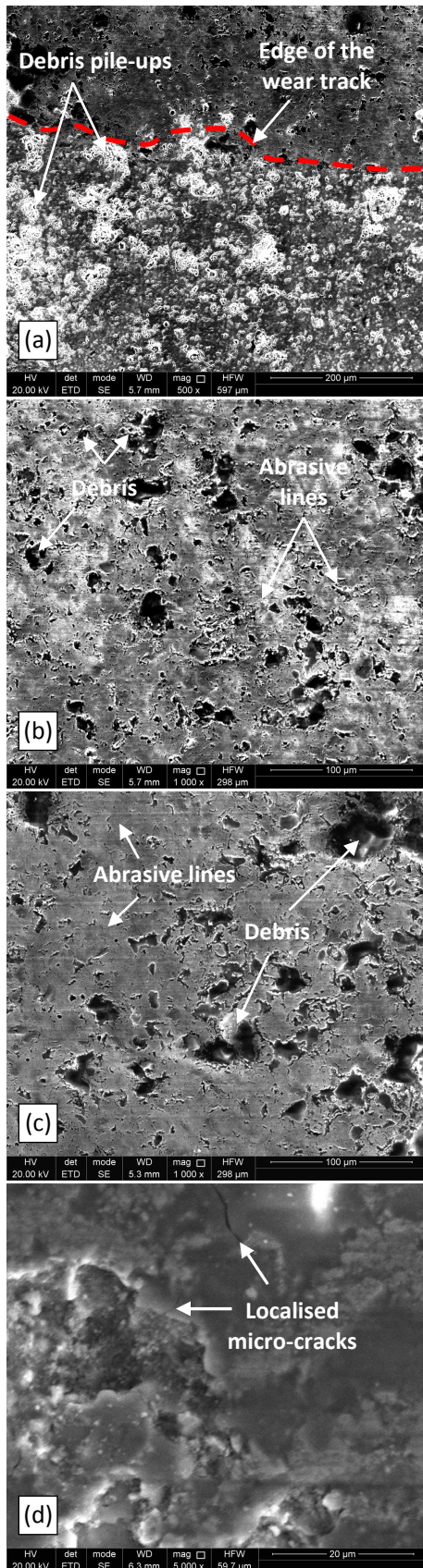


Figure 5. Indicative SEM images showing: (a) debris formation at the edge of chromia coating wear track, (b) abrasion lines and particle generation within chromia coating wear track, (c) abrasion and particle generation within titania coating wear track and (d) micro-crack formation within titania coating wear track

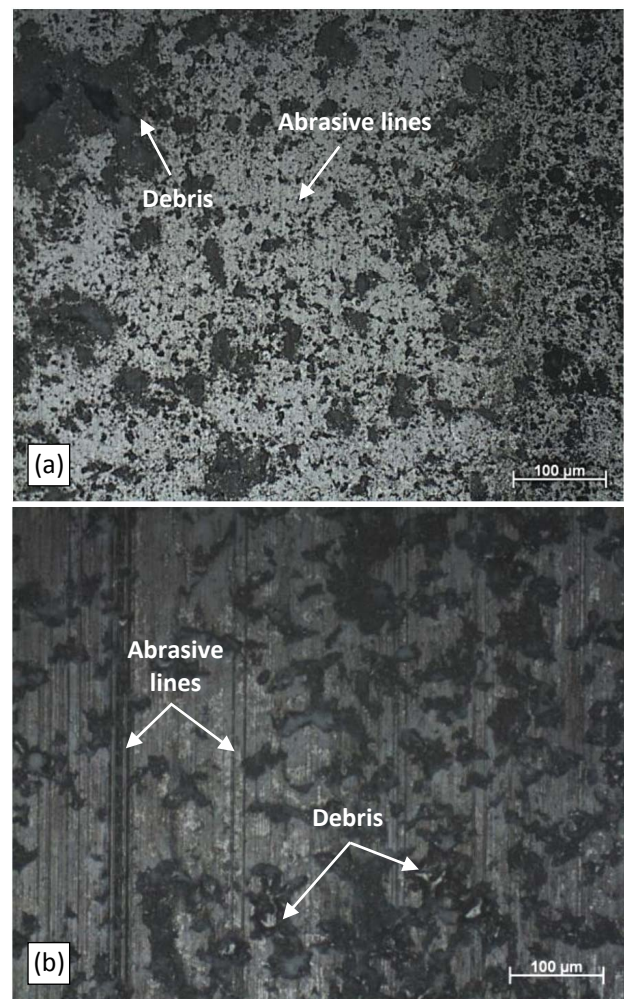


Figure 6. Indicative OM images within wear track of: (a) chromia coating and (b) titania coating

To explore the applicability of these thermally sprayed coatings under abrasive conditions, a comparison of friction (average coefficient of friction per cycle at the steady-state conditions for the triplicate tests) and wear (average wear depth obtained from triplicate tests) results was done with some widely used industrial materials and coatings (Fig. 7). From this comparison, it can be seen that the ceramic-based coatings have comparable if not better tribological properties for the given conditions. In particular, chromia coating had comparable wear resistance to high-cost DLC and to hard Cr coatings (that contain hexavalent Cr and are being banned by the EU). Indeed, confocal imaging of the wear track on the chromia coating shows a limited wear depth (Fig. 8a), in comparison to e.g. the advanced Haynes alloy (Fig. 8b). In terms of friction, they are in the same range as most metallic materials alloys but have a smaller spread of values due to their higher wear resistance that results in a smaller particle generation in the contact. However, their frictional

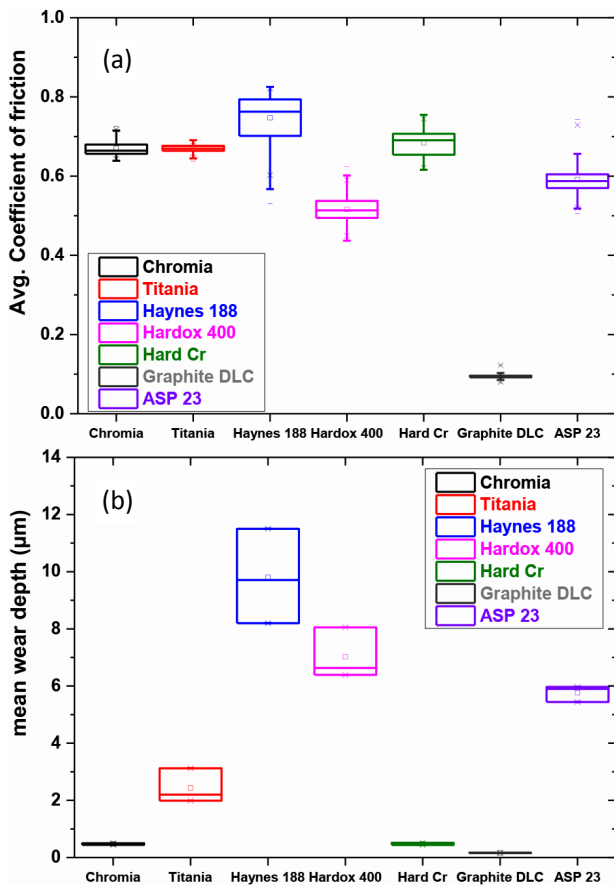


Figure 7. Comparison of average friction and wear between thermally sprayed titania and chromia coatings and industrial benchmarks (for the same test conditions, as described in the experimental part

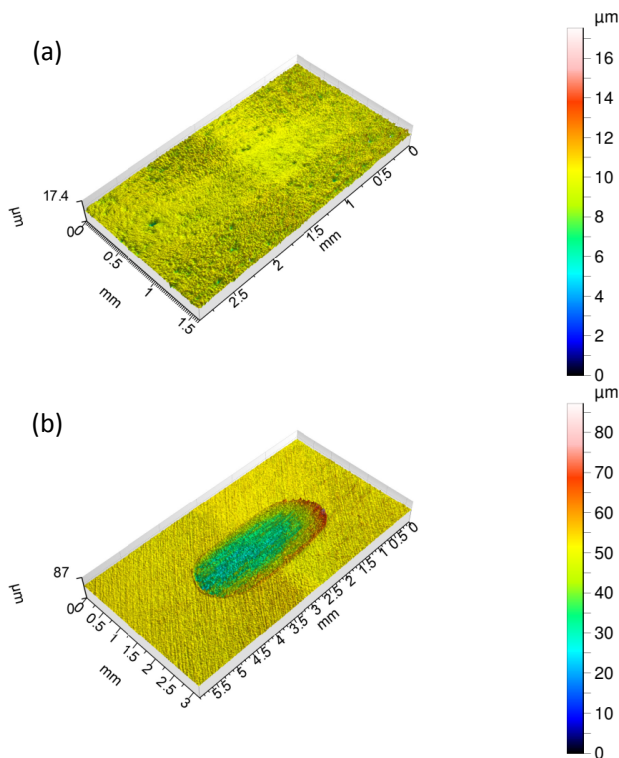


Figure 8. 3D confocal images of wear track, after sliding against corundum counter-body, on: (a) chromia coating and (b) Haynes 188 alloy

behaviour cannot be compared to state-of-the-art DLC coatings. This means that they can be potentially used for applications requiring high wear resistance, but not low friction without lubrication.

4. Conclusion

In this work, chromia and titania coatings were deposited via thermal spraying onto steel substrates. The coatings were dense and with very few cracks or flaws at the interface between the sprayed coating and the substrate, or between the sprayed splats, which indicates a satisfactory adhesion. In addition, no significant structural changes were observed between the sprayed powders and the deposited coating.

In terms of their tribological behaviour, both coatings had a similar average coefficient of friction vs. corundum, but a higher fluctuation of the friction force was observed for titania coating due to the higher density of debris particles within the contact. The main wear mechanisms were two-body abrasion due to the surface roughness of the counter-body material, as well as three-body abrasion due to the formation of debris at the interface. When compared to existing benchmarks, they have comparable if not better wear resistance and comparable friction (with the exception of the DLC reference).

References

- [1] P. Fauchais, A. Vardelle, B. Dussoubs, Quo vadis thermal spraying?, *Journal of Thermal Spray Technology*, Vol. 10, No. 1, 2001, pp. 44-66, DOI: [10.1361/105996301770349510](https://doi.org/10.1361/105996301770349510)
- [2] D. Tejero-Martin, M. Rezvani Rad, A. McDonald, T. Hussain, Beyond traditional coatings: A review on thermal-sprayed functional and smart coatings, *Journal of Thermal Spray Technology*, Vol. 28, No. 4, 2019, pp. 598-644, DOI: [10.1007/s11666-019-00857-1](https://doi.org/10.1007/s11666-019-00857-1)
- [3] M.R. Mrdak, A. Vencl, B.D. Nedeljkovic, M. Stanković, Influence of plasma spraying parameters on properties of thermal barrier coatings, *Materials Science and Technology*, Vol. 29, No. 5, 2013, pp. 559-567, DOI: [10.1179/1743284712Y.0000000193](https://doi.org/10.1179/1743284712Y.0000000193)
- [4] A. Vencl, Tribological behavior of ferrous-based APS coatings under dry sliding conditions, *Journal of Thermal Spray Technology*, Vol. 24, No. 4, 2015, pp. 671-682, DOI: [10.1007/s11666-014-0202-2](https://doi.org/10.1007/s11666-014-0202-2)

- [5] M. Gardon, J.M. Guilemany, Milestones in functional titanium dioxide thermal spray coatings: A review, *Journal of Thermal Spray Technology*, Vol. 23, No. 4, 2014, pp. 577-595, DOI: [10.1007/s11666-014-0066-5](https://doi.org/10.1007/s11666-014-0066-5)
- [6] S. Singh, C.C. Berndt, R.K. Singh Raman, H. Singh, A.S.M. Ang, Applications and developments of thermal spray coatings for the iron and steel industry, *Materials*, Vol. 16, No. 2, 2023, Paper 516, DOI: [10.3390/ma16020516](https://doi.org/10.3390/ma16020516)
- [7] A. Vencel, B. Katavić, D. Marković, M. Ristić, B. Gligorijević, The tribological performance of hardfaced/thermal sprayed coatings for increasing the wear resistance of ventilation mill working parts, *Tribology in Industry*, Vol. 37, No. 3, 2015, pp. 320-329.
- [8] G. Bolelli, Replacement of hard chromium plating by thermal spraying – problems, solutions and possible future approaches, *Surface Engineering*, Vol. 25, No. 4, 2009, pp. 263-269, DOI: [10.1179/174329409X373729](https://doi.org/10.1179/174329409X373729)
- [9] E.P. Georgiou, D. Drees, G. Timmermans, A. Zoikis-Karathanasis, M. Pérez-Fernández, L. Magagnin, J.-P. Celis, High performance accelerated tests to evaluate hard Cr replacements for hydraulic cylinders, *Coatings*, Vol. 11, No. 12, 2021, Paper 1511, DOI: [10.3390/coatings11121511](https://doi.org/10.3390/coatings11121511)
- [10] A.K. Basak, J.-P. Celis, M. Vardavoulias, P. Matteazzi, Abrasive wear of nanostructured cermet coatings in dry and slurry conditions, *International Journal of Refractory Metals and Hard Materials*, Vol. 100, 2021, Paper 105638, DOI: [10.1016/j.ijrmhm.2021.105638](https://doi.org/10.1016/j.ijrmhm.2021.105638)
- [11] E.M. Leivo, M.S. Vippola, P.P.A. Sorsa, P.M.J. Vuoristo, T.A. Mäntylä, Wear and corrosion properties of plasma sprayed Al_2O_3 and Cr_2O_3 coatings sealed by aluminum phosphates, *Journal of Thermal Spray Technology*, Vol. 6, No. 2, 1997, pp. 205-210, DOI: [10.1007/s11666-997-0014-8](https://doi.org/10.1007/s11666-997-0014-8)
- [12] R.A. Miller, Current status of thermal barrier coatings – An overview, *Surface and Coatings Technology*, Vol. 30, No. 1, 1987, pp. 1-11, DOI: [10.1016/0257-8972\(87\)90003-X](https://doi.org/10.1016/0257-8972(87)90003-X)
- [13] E.J. Gildersleeve V V, V. Viswanathan, M.J. Lance, J.A. Haynes, B.A. Pint, S. Sampath, Role of bond coat processing methods on the durability of plasma sprayed thermal barrier systems, *Surface and Coatings Technology*, Vol. 375, 2019, pp. 782-792, DOI: [10.1016/j.surfcoat.2019.07.065](https://doi.org/10.1016/j.surfcoat.2019.07.065)
- [14] X. Pang, K. Gao, A.A. Volinsky, Microstructure and mechanical properties of chromium oxide coatings, *Journal of Materials Research*, Vol. 22, No. 12, 2007, pp. 3531-3537, DOI: [10.1557/JMR.2007.0445](https://doi.org/10.1557/JMR.2007.0445)
- [15] R. Jaworski, L. Pawlowski, C. Pierlot, F. Roudet, S. Kozerski, F. Petit, Recent developments in suspension plasma sprayed titanium oxide and hydroxyapatite coatings, *Journal of Thermal Spray Technology*, Vol. 19, No. 1-2, 2010, pp. 240-247, DOI: [10.1007/s11666-009-9425-z](https://doi.org/10.1007/s11666-009-9425-z)
- [16] A. Koutsomichalis, A. Lontos, G. Loukas, M. Vardavoulias, N. Vaxevanidis, Fatigue behaviour of plasma sprayed titania and chromia coatings, *MATEC Web of Conferences*, Vol. 349, 2021, Paper 02009, DOI: [10.1051/mateconf/202134902009](https://doi.org/10.1051/mateconf/202134902009)
- [17] M. Hakovirta, J. Salo, A. Anttila, R. Lappalainen, Graphite particles in the diamond-like a-C films prepared with the pulsed arc-discharge method, *Diamond and Related Materials*, Vol. 4, No. 12, 1995, pp. 1335-1339, DOI: [10.1016/0925-9635\(95\)00313-4](https://doi.org/10.1016/0925-9635(95)00313-4)
- [18] E.P. Georgiou, D. Drees, S. Dosta, P. Matteazzi, J. Kusinski, J.-P. Celis, Wear evaluation of nanostructured Ti cermets for joint reconstruction, *Biotribology*, Vol. 11, 2017, pp. 44-50, DOI: [10.1016/j.biotri.2017.03.007](https://doi.org/10.1016/j.biotri.2017.03.007)
- [19] G. Bolelli, V. Cannillo, L. Lusvarghi, T. Manfredini, Wear behaviour of thermally sprayed ceramic oxide coatings, *Wear*, Vol. 261, No. 11-12, 2006, pp. 1298-1315, DOI: [10.1016/j.wear.2006.03.023](https://doi.org/10.1016/j.wear.2006.03.023)
- [20] P.N. Bogdanovich, Fatigue wear of materials under dynamic contact loading, *Journal of Friction and Wear*, Vol. 34, No. 5, 2013, pp. 349-357, DOI: [10.3103/S1068366613050036](https://doi.org/10.3103/S1068366613050036)